Applied Physics Letters

Dynamic response and roughening of ferroelectric domain walls driven at planar electrode edges

Cite as: Appl. Phys. Lett. **119**, 242903 (2021); https://doi.org/10.1063/5.0069920
Submitted: 02 September 2021 • Accepted: 02 November 2021 • Published Online: 14 December 2021

Guillaume Rapin, Sophia Ehrensperger, Cédric Blaser, et al.

Applied Physics Letters ARTICLE scitation.org/journal/apl

Dynamic response and roughening of ferroelectric domain walls driven at planar electrode edges

Cite as: Appl. Phys. Lett. **119**, 242903 (2021); doi: 10.1063/5.0069920
Submitted: 2 September 2021 · Accepted: 2 November 2021 ·
Published Online: 14 December 2021

View Online Export Citation CrossMark

Guillaume Rapin,[a] Sophia Ehrensperger,[b] Cédric Blaser,[c] Nirvana Caballero,[d] and Patrycja Paruch[e]

AFFILIATIONS

Department of Quantum Matter Physics, University of Geneva, 1211 Geneva, Switzerland

[a]guillaume.rapin@unige.ch
[b]**Present address**: DACM, State of Geneva, Switzerland.
[c]**Present address**: Federal Institute of Metrology METAS, Switzerland.
[d]nirvana.caballero@unige.ch
[e]**Author to whom correspondence should be addressed:** patrycja.paruch@unige.ch

ABSTRACT

Understanding and controlling the motion, stability, and equilibrium configuration of ferroelectric domain walls is key for their integration into potential nanoelectronic applications, such as ferroelectric racetrack memories. Using piezoresponse force microscopy, we analyze the growth and roughness of ferroelectric domains in epitaxial thin film $Pb(Zr_{0.2}Ti_{0.8})O_3$, driven by the electric fields at straight edges of planar electrodes at two different temperatures. This device relevant geometry allows us to confirm that the domain walls are well described as one-dimensional monoaffine elastic interfaces driven in random-bond disorder. However, we observe a progressive increase in roughness as initially flat domain walls move through the disorder landscape, which could prove a significant limiting factor for racetrack-type memories using ferroelectrics.

Ferroelectric materials, in which thin domain walls separate electrically reconfigurable domains with different polarization orientation, are widely used in sensing, actuation, nonlinear optics, and information storage applications.[1–4] Recent research has focused on emergent structural and functional properties of these domain walls[5–8] and their potential integration as active nanoelectronic device components.[9–11] For all such present and future applications, a detailed understanding of the fundamental physics underlying domain nucleation, growth, stability, and equilibrium configuration is essential.

In this context, a useful approach allowing a predictive description of the motion and geometric properties of domain walls is to model them as elastic interfaces in a disordered medium.[12,13] This general statistical physics framework allows common features in systems as diverse as flux lines in type II superconductors,[14] propagating fractures,[15] and proliferating cell fronts[16–18] to be compared. The behavior of such systems is governed by the competition between elasticity, which tends to flatten the interface, and fluctuations in the potential energy landscape resulting from the disorder, which allows pinning. This competition leads to a self-affine equilibrium roughness configuration, whose characteristic power-law scaling is related to the dimensionality of the system and the type of disorder. When driven by an external force, elastic disordered systems present a complex and highly nonlinear dynamic response, with a thermally activated subcritical creep regime and depinning when sufficiently high forces are applied.

In ferroelectrics, fundamental studies of roughness, memory effects, creep and depinning dynamics, and their characteristic avalanche statistics[19–24] have led to the implementation of a wide range of prototype nanoelectronic devices based on domain walls, focusing, in particular, on racetrack-type memory applications.[25–28] However, while in most device geometries, the domain walls are driven by an electric field applied in a planar capacitor configuration,[29–32] and in many fundamental studies, the dynamic response is both induced and imaged using scanning probe microscopy (SPM). In such studies, the extremely local application of a highly inhomogeneous electric field[33] can provoke significant electrochemical effects,[34] strongly dependent on both the polarization orientation and switching history of the ferroelectric.[35] For comparison with theoretical models of a straight linear interface in equilibrium with the native disorder present in the sample, and for more direct assessment of what happens in device-relevant

geometries, a useful alternative would be to exploit the nanoscale resolution of SPM for imaging, but to apply the external field using the straight edges of patterned macroscale electrodes. Such a protocol would establish a well-defined initial domain wall position, determined by the electrode geometry, and allow the domain walls to subsequently move away from the electrode edge and into the pristine region aside from it, reflective of the disorder potential landscape established during sample growth and unperturbed by electrochemical effects of domain writing using a biased tip. While pairs of surface electrodes can be used to establish an electric field oriented in the film plane to drive the switching of in-plane polarization components,[36,37] switching out-of-plane polarization components requires an electric field perpendicular to the film plane.

Here, we report on such a study, following domain wall dynamics and roughness of initially flat domain wall segments in $Pb(Zr_{0.2}Ti_{0.8})O_3$ thin films, driven by the fringing electric fields at the edges of straight patterned electrodes, as schematically illustrated in Fig. 1(a). We find that the domain walls are well described as monoaffine one-dimensional elastic interfaces in random bond disorder, with measurements at both 23 and 100 °C, demonstrating the importance of thermal activation in the creep regime and allowing us to extract the value of the creep exponent $\mu = 0.21 \pm 0.02$ with very high precision. We observe a progressive roughening of the domain walls as they move away from the electrode edges, with the roughness exponent increasing from $\zeta = 0.5$–0.6 to $\zeta = 0.7$–0.8, suggesting a qualitative difference between the disorder potential landscape of the as-grown sample and after high electric field application. This picture is compatible with observations in numerical simulations of interfaces in a Ginzburg–Landau model.[38] The observed roughening of the domain walls, which increases their effective width, may have significant consequences for the use of ferroelectrics in racetrack memory applications.

All measurements were performed on a ∼270 nm $Pb(Zr_{0.2}Ti_{0.8})O_3$ thin film, epitaxially grown with a 35 nm $SrRuO_3$ back electrode on (001) oriented single crystal $SrTiO_3$ by off-axis RF magnetron sputtering.[39] As detailed in the supplementary material, the film shows high crystalline and surface quality and presents an out-of-plane up-oriented monodomain polarization. 50 nm Au/5 nm Ti top electrodes with extended straight-edged sections were deposited by e-beam evaporation after photolithographic patterning. 10 V pulses of varying duration were applied to selected electrodes using ZN50R-10-BeCu needle contacts in a Lakeshore cryogenic probe station to induce polarization switching under the electrode in a standard parallel plate capacitor geometry, followed by the outward growth of the down-polarized domains at the electrode edges, driven by the exponentially decreasing out-of-plane component of the capacitor fringing field. To examine the effects of thermal activation, this polarization switching was carried out at 23 °C and 100 °C. The resulting domain configuration was imaged by piezoresponse force microscopy (PFM) in ambient conditions and analyzed with the Hystorian materials science data analysis package[40] to extract the position and follow the evolution of the 180° domain walls.

For short switching pulses, we initially observe the presence of small discontinuous down-polarized regions along the electrode edge, which coalesce into a continuous and progressively wider stripe domains when longer writing pulses are applied (see the supplementary material for PFM phase data), and the domain walls move further away from the electrode into the up-polarized bulk of the sample. From the images of the growing domains, we extract the transverse displacement $u(z, t)$ along the longitudinal coordinate z of the domain walls with respect to the electrode edge for a given switching pulse duration t, as shown in Fig. 1(b). The average domain width $\langle u(z,t)\rangle$, obtained by averaging $u(z, t)$ across a minimum of ten separate images from at least four independent electrodes, increases logarithmically with the switching pulse duration, as can be seen in Fig. 1(c). While the process is qualitatively similar, we observe significantly earlier onset and faster rates of domain growth at the higher temperature. From these measurements, we extract the domain wall velocity as the

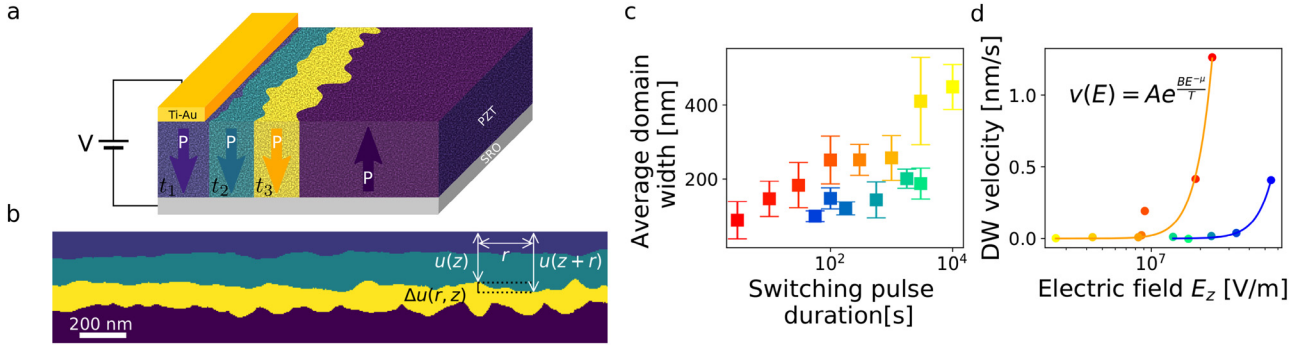

FIG. 1. Dynamics of domain walls at electrode edges. (a) Schematic representation of the measurement geometry, with the outward growth of a down-polarized stripe domain (blue, teal, and yellow), driven by the out-of-plane component of the fringing electric fields between the surface Ti–Au electrodes and the $SrRuO_3$ bottom electrode into the pristine up-polarized as-grown region of the sample (aubergine). (b) Composite illustration of the displacement $u(z)$ of the 180° domain wall with respect to the electrode edge, obtained from PFM phase images taken after the application of 10 V writing pulses for 3 (blue), 30 (teal), and 300 s (yellow) to Au/Ti electrodes patterned on a $Pb(Zr_{0.2}Ti_{0.8})O_3$ thin film at 100 °C. Initially relatively flat, the down-polarized domains grow outward from the electrode edge into the up-polarized as-grown regions of the film (aubergine) with increasing domain wall roughness, which can be quantified via the correlation of the relative displacements $\Delta u(r, z) = u(z) - u(z + r)$ measured between pairs of points separated by a distance r. (c) The average width of the growing domains increases logarithmically with increased switching pulse duration. (d) Domain wall velocity as a function of the out-of-plane component of the electric field at the edge of the electrode, showing a highly nonlinear dependence consistent with a creep process $v(E) = e^{\frac{-U_c}{k_B T}\left(\frac{E_c}{E}\right)^{\mu}}$. Comparison between room temperature (23 °C, blue–green color scale) and high temperature (100 °C, red–yellow color scale) measurements shows the significant effects of thermal activation characteristic of creep dynamics. We use the same color scale in (c) and (d) to show the correspondence between points in both plots.

increase in the average domain width $\langle u(z,t_2)\rangle - \langle u(z,t_1)\rangle$ over the interval between two sequential writing times $t_2 - t_1$, and correlate it with the out-of-plane electric field E_z at the edge of the electrode, obtained via Comsol modeling (as detailed in the supplementary material). We find a highly nonlinear dynamic response, which can be very well described as a creep process-the very slow, thermally activated dynamics for a subcritical driving force, characterized by jerky, stochastic jumps of an interface between different local minima in a highly heterogeneous potential energy landscape,

$$v(E) = e^{\frac{-U_c}{k_B T}\left(\frac{E_c}{E}\right)^{\mu}}, \tag{1}$$

where U_c is the characteristic energy barrier, T is the temperature, k_B is the Boltzmann constant, E is the applied electric field driving domain wall motion, and E_c is the critical field for depinning. Importantly, since fitting is performed self-consistently on the full dataset for both temperatures, a far more precise estimate of the dynamic exponent $\mu = 0.21 \pm 0.02$ can be obtained (as detailed in the supplementary material) than in previous studies.[19,21]

During the growth of the stripe domain, we also observe a pronounced evolution of their geometric configuration. As shown in Fig. 1(b), initially relatively flat domain walls near the electrode edges roughen visibly as they move progressively further away. This roughening can be quantified by examining the relative displacements $\Delta u(r,z) = u(z) - u(z+r)$ between two points along the wall separated by a distance r. By extracting the correlation function of these relative displacements

$$B(r,t) = \overline{\langle |\Delta u(r,t)|^2 \rangle} \sim r^{2\zeta}, \tag{2}$$

where $\langle \ldots \rangle$ and $\overline{\ldots}$ signify the average over different z values for a single domain wall segment, and the average over different realizations of disorder, respectively. We find overall a similar level of roughness for the domain walls driven at 23 °C [Fig. 2(a)] and 100 °C [Fig. 2(b)], comparable to previous reports of roughening at SPM-tip-patterned ferroelectric domain walls in $Pb(Zr_{0.2}Ti_{0.8})O_3$ PZT films subjected to thermal heat– quench cycles.[20] At both 23 °C and 100 °C, we find that the domain walls driven by the shortest switching pulses show the expected power-law scaling growth of $B(r)$ only at short lengthscales r up to 40–50 nm, followed by an apparent saturation reflecting their essentially flat nature at large lengthscales and initial times.[41,42] For longer writing times, $B(r)$ increases, and, particularly at the higher temperature, the power-law scaling region appears to extend somewhat further to over 200 nm. This behavior indicates that the electrode edge does not have a significant effect on the domain wall roughness exponents.

To further confirm these observations and compare the scaling exponents extracted with both approaches, we also carried out a reciprocal space analysis of the roughness, extracting the structure factor,

$$S(q,t) = \overline{\langle (\tilde{u}(q,t)\tilde{u}(-q,t))^n \rangle}, \tag{3}$$

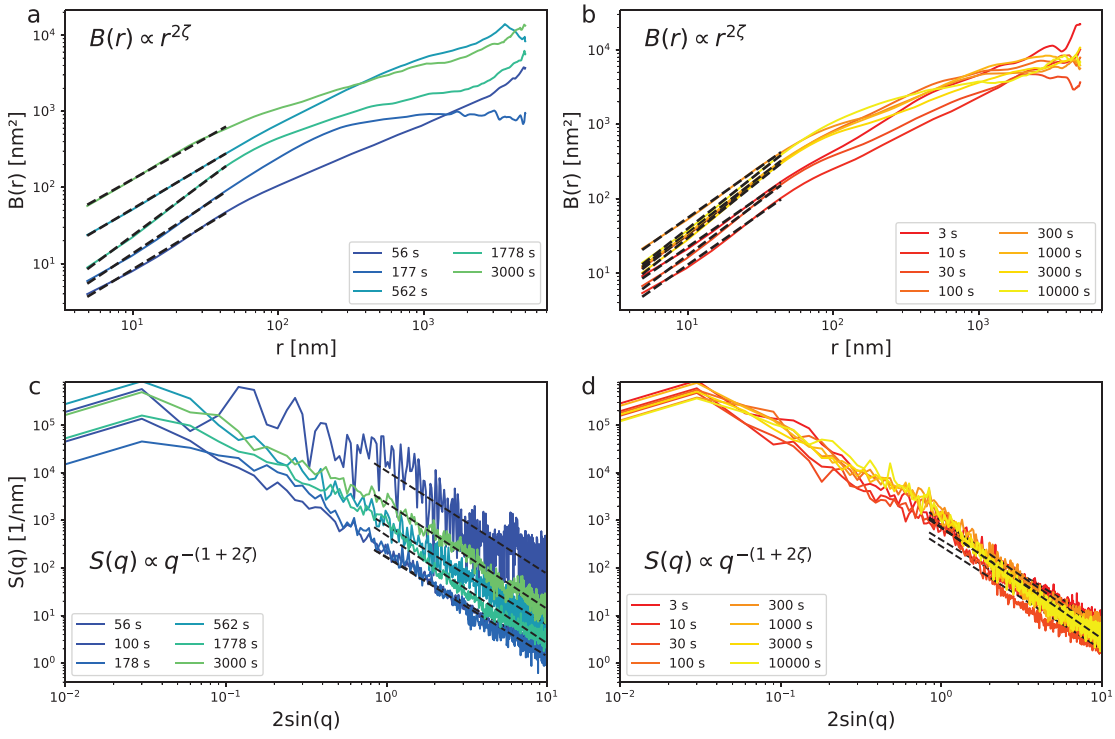

FIG. 2. Evolution of domain wall roughness during domain growth. Averaged roughness correlation function $B(r) = \langle |\Delta u(r,z)|^2 \rangle$ of domain walls written with pulse times ranging between 56 and 3000 s for 23 °C (a) and between 3 and 10 000 s for 100 °C (b), showing power law scaling $B(r) \sim r^{2\zeta}$ at short lengthscales r. Averaged structure factor $S(q) = \overline{\langle (\tilde{u}(q,t)\tilde{u}(-q,t))^n \rangle}$ of domain walls written with pulse times ranging between 56 and 3000 s for 23 °C (c) and between 3 and 10 000 s for 100 °C (d), showing power law scaling $S(q) \propto q^{-(1+2\zeta)}$ at large reciprocal lengthscales q. Fitting (black dashed lines) allows the characteristic roughness exponent ζ to be extracted from both real space and reciprocal space analysis.

where $\tilde{u}(q,t)$ is the Fourier transform of the displacement field, which defines the domain wall position,

$$\tilde{u}(q,t) = \frac{1}{L}\int dz\, u(z,t)e^{-iqz}. \quad (4)$$

Although $B(r,t)$ and $S(q,t)$ are related, containing the same geometric information about the domain wall roughness,

$$B(r,t) = \int \frac{dz}{\pi}[1-\cos(qr)]S(q,t), \quad (5)$$

the latter provides more reliable estimates of the roughness exponent value when sufficient statistics are available.[43] As shown in Figs. 2(d) and 2(e), we observe the expected power-law scaling of the structure factor $S(q) \propto q^{-(1+2\zeta)}$ at high reciprocal lengthscales q for the domain walls driven at 23 °C and 100 °C.

The roughness exponent ζ, whose value depends on the dimensionality of the system, the nature of the disorder potential, and the range of the elastic interactions can then be obtained by fitting this characteristic power-law scaling of $B(r)$ and $S(q)$. We find that the roughness exponents obtained from both the real space and reciprocal space analysis are in excellent agreement, although the latter consistently gives slightly lower values. As can be seen in Fig. 3(a), at room temperature, ζ values cluster uniformly around 0.5–0.6 but increase to 0.7–0.8 for long switching pulse duration at the higher temperature.

Multiscaling analysis of the probability distribution function of relative displacements following[15,44] (detailed in the supplementary material) confirms that the observed scaling appears to be monoaffine, as expected for elastic interfaces subject to weak collective pinning by random disorder[45–47] rather than multiaffine.[41,48,49]

These observations of ferroelectric domain wall roughness and dynamics in our specific measurement geometry reveal a number of important features. First, by comparing domain walls driven at 23 °C and 100 °C, we explicitly confirm the very significant role of thermal activation during creep motion, with speeds up to two orders of magnitude higher observed for comparable electric fields at the higher temperatures, an effect that is particularly important at low fields. This thermal activation allows a much larger stripe domain to grow for a given switching pulse duration, in spite of the exponentially decreasing magnitude of the out-of-plane component of the electric field as one moves further away from the electrode edge. Second, the very different aspect presented by the domain walls in the immediate vicinity of and furthest away from the electrode edges, with over twofold increase in roughness $B(r)$ and an evolution of the roughness exponent ζ from ~0.5 to ~0.8, points toward qualitative differences in the disorder potential landscape in the two cases.

Indeed, past studies of the effects of high intensity electric fields applied via an SPM tip demonstrated that polarization reversal can be accompanied by the injection and reorganization of charged defects, long-lasting electrochemical changes on the ferroelectric surface, and even significant material degradation for the highest field intensity.[34,35,50] The resulting patterned domains commonly show marked pinning of domain walls at their initial position, even after subsequent field application or heating.[20,24] We believe that the strong electric field right under the electrode and at its edge, comparable to that applied under a biased SPM tip,[33,39] has similar effects in our sample.

We note, moreover, that the relatively flat geometry of the domain walls in the immediate vicinity of the electrode edges, in spite of the higher electric field intensity, suggests the system is not simply in a depinning regime, where, in fact, higher growth of domain wall roughness may be expected.[51,52] However, as the domain walls progressively move away from the electrodes into the region of decreasing electric field intensity, their growing roughness, increasing roughness exponent values, and the extension of the power-law scaling region to higher r suggest that here the system is more effectively relaxing toward equilibrium with the pristine disorder potential landscape of the as-grown sample.

Values of the roughness exponent ζ in the 0.6–0.7 range had previously been observed in for both artificial and naturally occurring domain walls in $Pb(Zr_{0.2}Ti_{0.8})O_3$,[44,53] and together with dynamic exponent μ of 0.21 would be compatible with the theoretical predictions for 1-dimensional elastic interfaces in random bond disorder.[54,55] The random bond disorder at the origin of the observed domain wall

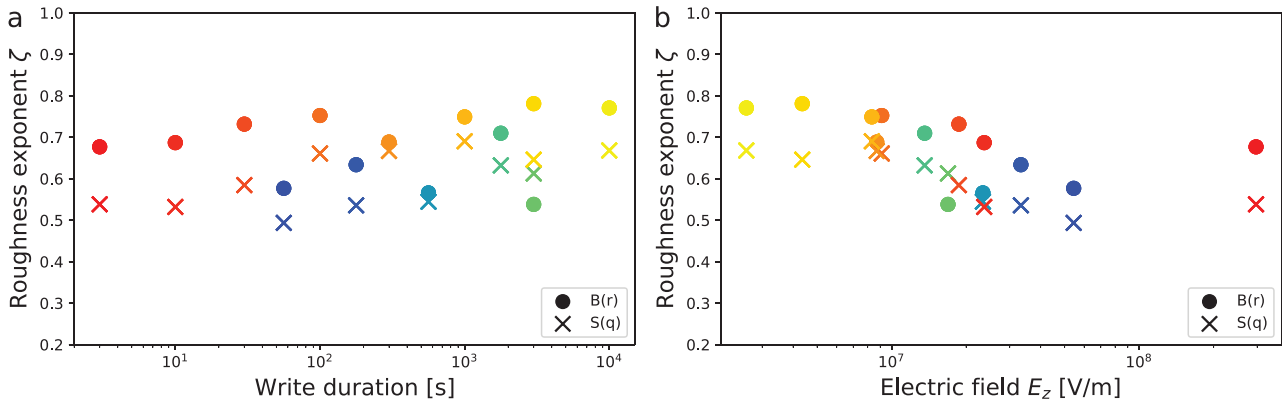

FIG. 3. Evolution of the domain wall roughness exponent during domain growth. ζ values extracted from fitting power-law scaling of $B(r)$ (circles) and $S(q)$ (crosses), and followed as a function of (a) the switching pulse duration and (b) the out-of-plane electric field. While at room temperature (23 °C, blue–green color scale), ζ values cluster uniformly around 0.5–0.6, and at high temperature (100 °C, red–yellow color scale), ζ values increase to 0.7–0.8 for long switching pulse duration, as the domain walls move further away from the electrode edges into a region of lower electric field intensity. The color scales are used to help the reader to assess the correspondence between points in (a) and (b).

roughening can be interpreted as site-to-site fluctuations in the energy barrier that the polarization has to overcome during 180° switching.[42] These fluctuations can be related to uncharged defects in the crystalline order or locally varying surface morphology.[13,56]

Our observations of progressively increasing roughness as initially flat domain walls move through the disorder landscape are particularly pertinent for potential ferroelectric-based racetrack memory applications,[25–28] where the resulting broadening of the information-carrying region could prove a significant limiting factor. A possible solution would be to focus on ferroelastic ferroelectric domain walls,[57–59] where additional strain terms could help maintain straighter walls.

See the supplementary material for a representative selection of PFM phase and amplitude images of domain growth at 23 and 100 °C, details of electric field modeling, details of creep dynamics fitting to extract μ, and the full multiscaling analysis of the domain wall geometry at 23 and 100 °C.

This work was partially supported by Division II of the Swiss National Science Foundation under Project No. 200021_178782. N.C. acknowledges support from the Federal Commission for Scholarships for Foreign Students for the Swiss Government Excellence Scholarship (ESKAS No. 2018.0636).

AUTHOR DECLARATIONS

Conflict of Interest

The authors declare no competing interest.

Author Contributions

P.P. designed and supervised the work. S.E. performed the PFM switching measurements and carried out preliminary analysis with assistance from C.B. and G.R. carried out the full multiscaling data analysis. G.R., N.C., and P.P. wrote the manuscript. All authors contributed to the scientific discussion and manuscript revisions. G.R. and N.C. contributed equally to this work.

DATA AVAILABILITY

The data that support the findings of this study are openly available in Yareta at http://doi.org/10.26037/yareta:pmummlrfbneihiwchlsejykinu.

REFERENCES

[1]P. Muralt, J. Micromech. Microeng. **10**, 136 (2000).
[2]M. Dawber, K. Rabe, and J. Scott, Re. Mod. Phys. **77**, 1083 (2005).
[3]L. Qi, S. Ruan, and Y.-J. Zeng, Adv. Mater. **33**, 2005098 (2021).
[4]S. Hong, O. Auciello, and D. Wouters, *Emerging Non-Volatile Memories* (Springer, 2014).
[5]S. Cherifi-Hertel, H. Bulou, R. Hertel, G. Taupier, K. D. H. Dorkenoo, C. Andreas, J. Guyonnet, I. Gaponenko, K. Gallo, and P. Paruch, Nat. Commun. **8**, 15768 (2017).
[6]D. Meier, J. Phys. **27**, 463003 (2015).
[7]J. Seidel, L. W. Martin, Q. He, Q. Zhan, Y.-H. Chu, A. Rother, M. E. Hawkridge, P. Maksymovych, P. Yu, M. Gajek, N. Balke, S. V. Kalinin, S. Gemming, F. Want, G. Catalan, J. F. Scott, N. A. Spaldin, J. Orenstein, and R. Ramesh, Nat. Mater. **8**, 229 (2009).
[8]J. Guyonnet, I. Gaponenko, S. Gariglio, and P. Paruch, Adv. Mater. **23**, 5377 (2011).
[9]E. K. H. Salje, ChemPhysChem **11**, 940 (2010).
[10]G. Catalan, J. Seidel, R. Ramesh, and J. F. Scott, Rev. Mod. Phys. **84**, 119 (2012).
[11]P. Sharma, P. Schoenherr, and J. Seidel, Materials **12**, 2927 (2019).
[12]T. Giamarchi, A. B. Kolton, and A. Rosso, in *Jamming, Yielding and Irreversible Deformation in Condensed Matter*, edited by M. C. Miguel and J. M. Rubi (Springer-Verlag, Berlin, 2006), p. 91.
[13]P. Paruch and J. Guyonnet, C. R. Phys. **14**, 637 (2013).
[14]G. Blatter, M. V. Feigel'man, V. B. Geshkenbein, A. I. Larkin, and V. M. Vinokur, Rev. Mod. Phys. **66**, 1125 (1994).
[15]S. Santucci, K. J. Mäløy, A. Delaplace, J. Mathiesen, A. Hansen, J. O. H. Bakke, J. Schmittbuhl, L. Vanel, and R. Purusattam, Phys. Rev. E **75**, 016104 (2007).
[16]M. Huergo, M. Pasquale, A. Bolzán, A. Arvia, and P. González, Phys. Rev. E **82**, 031903 (2010).
[17]O. Chepizhko, C. Giampietro, E. Mastrapasqua, M. Nourazar, M. Ascagni, M. Sugni, U. Fascio, L. Leggio, C. Malinverno, G. Scita *et al.*, Proc. Natl. Acad. Sci. **113**, 11408 (2016).
[18]G. Rapin, N. Caballero, I. Gaponenko, B. Ziegler, A. Rawleigh, E. Moriggi, T. Giamarchi, S. A. Brown, and P. Paruch, Sci. Rep. **11**, 8869 (2021).
[19]P. Paruch, T. Giamarchi, and J.-M. Triscone, Phys. Rev. Lett. **94**, 197601 (2005).
[20]P. Paruch, A. B. Kolton, X. Hong, C. H. Ahn, and T. Giamarchi, Phys. Rev. B **85**, 214115 (2012).
[21]T. Tybell, P. Paruch, T. Giamarchi, and J.-M. Triscone, Phys. Rev. Lett. **89**, 097601 (2002).
[22]J. Y. Jo, S. M. Yang, T. H. Kim, H. N. Lee, J.-G. Yoon, S. Park, Y. Jo, M. H. Jung, and T. W. Noh, Phys. Rev. Lett. **102**, 045701 (2009).
[23]B. Casals, G. F. Nataf, D. Pesquera, and E. K. H. Salje, APL Mater. **8**, 011105 (2020).
[24]P. Tückmantel, I. Gaponenko, N. Caballero, J. C. Agar, L. W. Martin, T. Giamarchi, and P. Paruch, Phys. Rev. Lett. **126**, 117601 (2021).
[25]L. J. McGilly, P. Duding, L. Feign, A. K. Tagantseav, and N. Setter, Nat. Nanotechnol. **10**, 145 (2015).
[26]L. McGilly, L. Feigl, T. Sluka, P. Yudin, A. Tagantsev, and N. Setter, Nano Lett. **16**, 68 (2016).
[27]M. McMillen, R. G. P. McQuaid, S. C. Haire, C. D. McLaughlin, L. W. Chang, A. Schilling, and J. M. Gregg, Appl. Phys. Lett. **96**, 042904 (2010).
[28]R. G. P. McQuaid, L.-W. Chang, and J. M. Gregg, Nano Lett. **10**, 3566 (2010).
[29]S. Hong, E. L. Colla, E. Kim, D. V. Taylor, A. K. Tagantsev, P. Muralt, K. No, and N. Setter, J. Appl. Phys. **86**, 607 (1999).
[30]A. Gruverman, D. Wu, and J. F. Scott, Phys. Rev. Lett. **100**, 097601 (2008).
[31]R. G. McQuaid, M. P. Campbell, R. W. Whatmore, A. Kumar, and J. M. Gregg, Nat. Commun. **8**, 15105 (2017).
[32]J. P. V. McConville, H. Lu, B. Wang, Y. Tan, C. Cochard, M. Conroy, K. Moore, A. Harvey, U. Bangert, L.-Q. Chen, A. Gruverman, and J. M. Gregg, Adv. Funct. Mater. **30**, 2000109 (2020).
[33]C. Blaser and P. Paruch, New J. Phys. **17**, 013002 (2015).
[34]S. V. Kalinin, S. Jesse, A. Tselev, A. P. Baddorf, and N. Balke, ACS Nano **5**, 5683 (2011).
[35]N. Domingo, I. Gaponenko, K. Cordero-Edwards, N. Stucki, V. Pérez-Dieste, C. Escudero, E. Pach, A. Verdaguer, and P. Paruch, Nanoscale **11**, 17920 (2019).
[36]P. Sharma, D. Sando, Q. Zhang, X. Cheng, S. Prosandeev, R. Bulanadi, S. Prokhorenko, L. Bellaiche, L.-Q. Chen, V. Nagarajan, and J. Seidel, Adv. Funct. Mater. **29**, 1807523 (2019).
[37]J. G. M. Guy, C. Cochard, P. Aguado-Puente, E. Soergel, R. W. Whatmore, M. Conroy, K. Moore, E. Courtney, A. Harvey, U. Bangert, A. Kumar, R. G. P. McQuaid, and J. M. Gregg, Adv. Mater. **33**, 2008068 (2021).
[38]N. Caballero, J. Stat. Mech. **2021**, 103207.
[39]C. Blaser and P. Paruch, Appl. Phys. Lett. **101**, 142906 (2012).
[40]L. Musy, R. Bulanadi, I. Gaponenko, and P. Paruch, Ultramicroscopy **228**, 113345 (2021).
[41]A. B. Kolton, A. Rosso, and T. Giamarchi, Phys. Rev. Lett. **95**, 180604 (2005).
[42]N. Caballero, E. Agoritsas, V. Lecomte, and T. Giamarchi, Phys. Rev. B **102**, 104204 (2020).
[43]S. Bustingorry, J. Guyonnet, P. Paruch, and E. Agoritsas, J. Phys. **33**, 345001 (2021).

[44]J. Guyonnet, E. Agoritsas, S. Bustingorry, T. Giamarchi, and P. Paruch, Phys. Rev. Lett. **109**, 147601 (2012).
[45]T. Halpin-Healy, Phys. Rev. A **44**, R3415 (1991).
[46]M. Mézard and G. Parisi, J. Phys. I **1**, 809 (1991).
[47]A. Rosso, R. Santachiara, and W. Krauth, J. Stat. Mech. **2005**, L08001.
[48]T. Nattermann, Y. Shapir, and I. Vilfan, Phys. Rev. B **42**, 8577 (1990).
[49]A.-L. Barabasi, R. Bourbonnais, M. Jensen, J. Kertesz, T. Vicsek, and Y.-C. Zhang, Phys. Rev. A **45**, R6951 (1992).
[50]A. V. Ievlev, P. Maksymovych, M. Trassin, J. Seidel, R. Ramesh, S. V. Kalinin, and O. S. Ovchinnikova, ACS Appl. Mater. Interfaces **8**, 29588 (2016).
[51]J. M. López, M. A. Rodríguez, and R. Cuerno, Phys. Rev. E **56**, 3993 (1997).
[52]V. H. Purrello, J. L. Iguain, and A. B. Kolton, Phys. Rev. E **99**, 032105 (2019).
[53]N. A. Pertsev, D. A. Kiselev, I. K. Bdikin, M. Kosec, and A. L. Kholkin, J. Appl. Phys. **110**, 052001 (2011).
[54]T. Nattermann, Europhys. Lett. **4**, 1241 (1987).
[55]E. Agoritsas, V. Lecomte, and T. Giamarchi, Physica B **407**, 1725 (2012).
[56]G. Lu, S. Li, X. Ding, J. Sun, and E. K. Salje, Sci. Rep. **9**, 1328 (2019).
[57]J. F. Scott, A. Hershkovitz, Y. Ivry, H. Lu, A. Gruverman, and J. M. Gregg, Appl. Phys. Rev. **4**, 041104 (2017).
[58]E. K. H. Salje, J. Appl. Phys. **128**, 164104 (2020).
[59]M. Barzilay and Y. Ivry, Nanoscale **12**, 11136 (2020).